OPEN GEOMECHANICS

The role of disjoining pressure on the drying shrinkage of cementitious materials

Syeda Rahman [a] *& Zachary Grasley* [b]

[a] *Center for Transportation Research, University of Texas at Austin*

[b] *Department of Civil & Environmental Engineering, Texas A&M University.*

Published
11th October 2023
https://doi.org/10.5802/ogeo.14

Edited by
Chloé Arson
School of Civil and Environmental Engineering
Georgia Institute of Technology

Reviewed by
Ippei Maruyama
Graduate School of Engineering
University of Tokyo
Yida Zhang
Department of civil, Environmental and Architectural Engineering
University of Colorado Boulder
Abudushalamu Aili
Graduate School of Environmental Studies
Nagoya University

Correspondence
Syeda Rahman
Center for Transportation Research,
University of Texas at Austin
3925 W. Braker Ln., Austin, TX 78759
USA
syedarahman@utexas.edu

Open Geomechanics is member of the Centre Mersenne for Open Scientific Publishing

Abstract. Drying induced shrinkage is often attributed to two major mechanisms- capillary pressure in the bulk pore solution and disjoining pressure in the liquid film separating the vapor phase from the pore wall or separating solid surfaces in nanometric pores. There is sufficient ambiguity in literature regarding the relative contribution of these two mechanisms, as well as the means to quantify their contributions. The objective of this manuscript is to evaluate the contribution of disjoining pressure in the drying shrinkage of cementitious materials. An unconventional approach to determining disjoining pressure within the framework of continuum mechanics is presented. This approach utilizes the conservation of linear momentum to derive a generalized expression of the disjoining pressure from the Lorentz force vector. The expression suggests that disjoining pressure is essentially an osmotic pressure at the contact surfaces that counters the electrostatic contribution to linear momentum. The proposed theory accurately predicts measurements of osmotic pressure found in the literature for the swelling of charged bilayers in a dilute salt solution. Applied to the shrinkage problem, the theory suggests that shrinkage stress is induced by the reduction in the potential gradient between the liquid film and bulk solution from the reference (fully saturated) state. The reduction in the potential gradient is caused by an increase in the concentration of the solutes in the pore solution when liquid water is removed as the relative humidity decreases.

Keywords. Drying shrinkage, cementitious materials, capillary pressure, disjoining pressure

1. Introduction

Drying shrinkage is the volumetric contraction associated with the removal of water from the pore network of a porous body. When concrete is subject to drying, it can exhibit substantial cracking compromising its strength and durability. It is essential to understand mechanisms that drive drying shrinkage so that mitigation techniques to shrinkage induced damage can be developed. Once the drying process starts, the pore space consists of the bulk liquid and vapor space separated from the pore wall by a thin liquid film. Mechanisms that drive shrinkage in cementitious materials are generally attributed to capillary pressure in the bulk liquid and disjoining pressure in the thin liquid film separating the vapor phase from the pore wall or separating solid surfaces in nanometric pores. The concept of capillary pressure was first presented by Young [1805] and formulated by Laplace [1805] as

$$p^v - p^l = \frac{2\gamma}{r}, \tag{1}$$

where p^v is the vapor pressure, p^l is the liquid pressure, γ is the liquid-vapor surface tension, and r is the mean curvature of a liquid-vapor interface. Thomson [1871] (also known as Lord Kelvin) later demonstrated that the vapor pressure is suppressed above a curved liquid-vapor interface such that

$$\frac{2\gamma}{r} = -\frac{\rho^l RT}{m^v}\ln(RH), \tag{2}$$

where ρ^l is the density of the liquid water, m^v is the molar mass of water, R is the ideal gas constant, $RH = p^v/p^{v-sat}$ is the relative humidity of the vapor, where p^{v-sat} is the saturated vapor pressure, and T is the temperature. The combination of equations 1 and 2 yields the so-called Kelvin-Laplace equation according to

$$p^v - p^l = -\frac{\rho^l RT}{m^v}\ln(RH), \tag{3}$$

which relates the suppression of the vapor pressure to the pressure difference between the liquid and gaseous phases. Equation 3 is an important expression that has been utilized to model the drying shrinkage of cementitious materials. This equation may be readily modified to account for the presence of dissolved species, which is significant in pores of hydrated cement paste [Coussy, 2010a, Grasley and Leung, 2011].

Since equation 1 is derived by enforcing conservation of linear momentum across a stable curved interface separating the liquid and vapor phase, and existence of such a stable meniscus in single nanometer sized pores has been debated [Christenson, 1985, 1988, Fisher et al., 1981, Fisher and Israelachvili, 1981a,b, Yang et al., 2020], Beltzung and Wittmann [2005] question the importance of equation 3 for concrete and argue that capillary pressure is not a primary mechanism for drying shrinkage. Beltzung and Wittmann [2005] instead emphasize that only disjoining pressure is relevant in mature cement paste as most water is in pore space a few nanometers in diameter. Beltzung and Wittmann [2005] present the interaction of adsorbed and capillary condensed water in a narrow gap between a thin quartz plate and a supporting block as evidence that disjoining pressure is the dominant mechanism in the swelling of nanoporous materials. They show that as the relative humidity increases more than 55%, condensation occurs between the plates and the block and the separation between the solids increases. They argue that during desiccation structured water (adsorbed water films that cover cement hydrate surfaces) evaporates, disjoining pressure decreases, due to attractive forces surfaces come closer, and shrinkage occurs. The study also notes that dissolved ions contribute considerably to disjoining pressure by the hydration of ions or building up of electrical double layers. Several other studies investigating disjoining pressure with surface force apparatuses show that bulk concentrations of the dissolved ions have a pronounced influence on disjoining pressure [Churaev et al., 2000, Pashley, 1981a,b, Pashley and Quirk, 1984, Plassard et al., 2005].

Based on the work of Neimark et al. [2003] and Gor and Neimark [2010], Scherer [2015] stated that disjoining pressure is additive to the pressure given by equation 2 and can be combined together to express the capillary pressure,P_c, as

$$P_c = \pi(\delta) + \frac{2\gamma}{r-\delta} = -\frac{\rho^l RT}{m^v}\ln(RH), \tag{4}$$

where π is the disjoining pressure and a function of the thickness, δ, of the adsorbed layer of the liquid on the solid surface.

In a recent article, Rahman and Grasley [2017] showed that the disjoining pressure in a flat liquid film separating the vapor phase from the pore wall is in mechanical equilibrium with the vapor pressure and does not need to be considered separately (beyond the capillary pressure given in equation 3) for modeling drying shrinkage in the context of poroelastic deformation. This finding is in agreement with Derjaguin et al. [1987] who noted that the pressure within a thin liquid film separating a solid and vapor is expressed fully by equation 3, which unfortunately has also been referred to as disjoining pressure in [Derjaguin et al., 1987]. Furthermore, as far back as 1901, Lewis [1901] demonstrated that expressions like that in equation 3 may be derived without any presumption about the existence of a meniscus between the vapor and liquid phases.

Rahman and Grasley [2017] specifically derived equation 3 from conservation of energy principles via a Gibbs-Duhem type state equation to demonstrate that the capillary pressure expressed by equation 3 does not require presence of a meniscus. The implication is that equation 3 is applicable to shrinkage stress generated across the full range of relative humidity – not simply at levels where a defined capillary meniscus is present – and there is no additional disjoining pressure in the thin water film between solid particles and the vapor phase contributing to shrinkage. The explanation of the concrete shrinkage mechanism whereby solid surfaces separated by a thin liquid film come closer with decreasing disjoining pressure is also dubious as the pore size does not change considerably with respect to the reference state (unlike with clays, the change in pore sizes of concrete due to shrinkage strain is negligible). The question naturally

arises, then, as to whether disjoining pressure changes contribute to shrinkage at all. The ambiguous understanding of the contribution of disjoining pressure changes warrants reevaluation of the mechanisms driving drying shrinkage. The objective of this paper is to carefully evaluate disjoining pressure and understand its contribution in drying shrinkage within the framework of continuum mechanics. An expression of disjoining pressure is derived from the conservation of linear momentum – an approach that is unconventional versus that found in historical references. The final, derived expression is in complete agreement to the formulations found in literature but provides valuable insights in the context of drying shrinkage mechanisms of porous bodies like concrete.

2. Understanding disjoining pressure

The concept of disjoining pressure was first introduced by Derjaguin [Derjaguin and Kusakov, 1936, 1937], and his approach to modeling the phenomena has been utilized by numerous authors across myriad disciplines. The classical demonstration of disjoining pressure [Derjaguin and Kusakov, 1936, 1937] is an experiment that involves two parallel, atomically smooth plates in a liquid bath. The two plates are brought ever closer together while the force required to achieve a particular separation between the plates is recorded. As the plates become very close to each other, the force required to achieve the small separation may become very high; this force, normalized by the cross-sectional area of the plates, results in a 'pressure' that is greater than that of the bulk solution comprising the bath. The disjoining pressure for this type of problem is defined by Derjaguin et al. [1987] as the difference between the calculated pressure between the plates and that of the bulk solution.

Disjoining pressure exists in other nanoscale problems besides two solid surfaces separated by a thin layer of liquid [Basu and Sharma, 1996, Hu and Sun, 2013, Mate, 1992, Napari and Laaksonen, 2003, Sefiane, 2006]. As discussed by Derjaguin in the 1930s [Derjaguin and Kusakov, 1936, 1939, Derjaguin and Obukhov, 1936], a general definition of disjoining pressure in a thin liquid or gaseous interlayer is the difference between the component of the anisotropic (i.e., non-spherical) stress tensor normal to the interlayer thickness and the pressure in the bulk phase from which the interlayer is formed. It is a vital parameter in spreading of a liquid film on a solid surface and has important implications in many engineering applications including surface modification, heat transfer, lubrication, emulsion, and oil recovery [Basu and Sharma, 1996, Chatterjee et al., 2011, Chengara et al., 2004, Churaev et al., 1994, Kuchin et al., 2014, Langevin, 2000, Mate, 1992, Picano et al., 2001, Pushkarova and Horn, 2005, Starov et al., 1994, Stubenrauch and Von Klitzing, 2003].

In order to quantify the magnitude of the disjoining pressure in the liquid between two surfaces in close proximity, Derjaguin and Churaev [1978] used the approach of LANDAU and LIFSHITZ [1984] whereby a total stress tensor is quantified (i.e., the electrodynamic or electrostatic body forces are reduced to forces applied to the surface of a material volume, and then inserted directly into a single stress tensor). This approach of utilizing a total stress tensor arises out of the work of Maxwell [1954], whereby electric and magnetic forces on point charges were converted to continuous fields to formulate a conservation of linear momentum in terms of the divergence of the "Maxwell stress tensor" rather than in terms of the Lorentz force. Thus, the total stress tensor is the sum of the Cauchy (mechanical) stress tensor and a fictitious electrostatic (or, more generally, electromagnetic) 'stress' tensor. Since the total stress tensor is anisotropic due to the non-zero off-diagonal terms originating from the electrostatic stress tensor, such an approach of using the total stress tensor may inadvertently imply shear stresses are present in the interlayer liquid between two closely spaced surfaces. Liquids such as water are generally modeled via constitutive equations that invoke sphericity of the (Cauchy) stress tensor, and shear stresses are disallowed unless the inertia is non-zero. One could argue that the nature of water (and thus its constitutive behavior) is different in tight spaces such that the material behaves more solid-like and can sustain shear stresses (see Gibbs [1878]). However, disjoining forces have been measured in aqueous solutions when the spacing between the surfaces is relatively large (over 100 nm) compared to the diameter of a water molecule (less than 0.5 nm) [Horn et al., 1996, Pushkarova and Horn, 2005, 2008, Yaminsky et al., 2010]. Furthermore, one could imagine a gravitational field as being analogous to an electric field as both may be expressed as a body force. As is well known, a gravitational field does not induce shear stresses in static liquids, so why should a local electric field?

In order to deal with this question, let us reconsider the experiment first described by Derjaguin involving two parallel plates being brought into close proximity in a liquid bath as shown in Figure 1 and separate the Maxwell stress tensor from the Cauchy stress tensor. Furthermore, we use Lorentz (electrostatic) force vector instead of the equivalent Maxwell stress tensor. By considering Derjaguin's experiment, we show that the theory is conceptually sound when applied to the shrinkage of porous bodies. Further, despite the argument that solid surface spacing does not significantly change during the drying process of concrete, the illustration presented below provides new insight in interpreting the contribution of disjoining pressure in drying shrinkage of cementitious materials. In such a problem, let us first define a priori the Cauchy stress tensor ($\underline{\underline{\sigma}}$) of the interlayer liquid to be spherical such that

$$\underline{\underline{\sigma}} \equiv \begin{pmatrix} -p-\pi & 0 & 0 \\ 0 & -p-\pi & 0 \\ 0 & 0 & -p-\pi \end{pmatrix}, \tag{5}$$

where p is the pressure in the bulk liquid of the bath and π is any additional mechanical (Cauchy) pressure that exists within the interlayer liquid. The conservation of linear momentum may be expressed as

$$\rho \frac{d\underline{v}}{dt} = \operatorname{div}\left[\underline{\underline{\sigma}}\right] + \underline{f}, \tag{6}$$

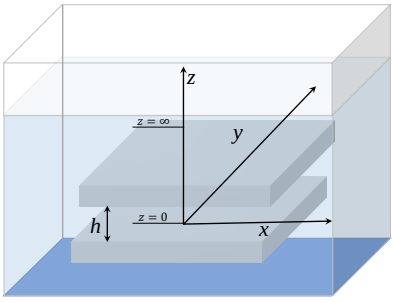

Figure 1. Diagram showing Derjaguin's experiment where two parallel plates are brought together in a liquid bath. A thin film of thickness h separates the two plates and exhibits an excess pressure relative to the bulk liquid.

where $\frac{d}{dt}$ is the material time derivative, $\underline{v}$ is the material velocity vector, ρ is the mass density, and $\underline{f}$ is the net body force. We may use superposition to break the force down such that $\underline{f} = \underline{f}_e + \underline{f}_{other}$ (where $\underline{f}_e$ is the body force due to electric fields and $\underline{f}_{other}$ refers to other body forces due to fields – like gravity – other than the electric field) to find

$$\rho \frac{d\underline{v}}{dt} = \operatorname{div}\left[\underline{\underline{\sigma}}\right] + \underline{f}_e + \underline{f}_{other}. \tag{7}$$

Based on the work of Coulomb on forces between charged particles, along with the notion of superposition of such forces and a suitable definition for the electrostatic[(1)] field vector ($\underline{E}$), one finds that the Lorentz force vector ($\underline{f}_e$) may be expressed by

$$\underline{f}_e = q_e \underline{E}, \tag{8}$$

where q_e is the charge density of the charged particles. If inertia and $\underline{f}_{other}$ are negligible, the conservation of linear momentum takes the form of[(2)]

$$\operatorname{div}\left[\underline{\underline{\sigma}}\right] = -\underline{f}_e = -q_e \underline{E}, \tag{9}$$

where

$$q_e = \sum \zeta_i e n_i, \tag{10}$$

is the total charge of the system carrying i ions and ζ_i is the valence of ith ion. Here, n_i is the number density of ionic species i, and $e = 1.602 \times 10^{-19}$C is the elementary protonic charge. The Nernst equation, providing the Boltzmann distribution of ions and defining the relationship between the ion number density and the electric potential, states that

$$n_i = n_0 \mathrm{e}^{-\zeta_i e(\psi - \psi_0)/kT}, \tag{11}$$

where n_0 is the number density of ions in the bulk solution, ψ is scalar electric potential, ψ_0 is the electrostatic potential in the bulk solution, and k is the Boltzmann constant. Equations 9 and 10 can be combined to give

$$\operatorname{div}\left[\underline{\underline{\sigma}}\right] = -\sum \zeta_i e n_i \underline{E}. \tag{12}$$

Conservation of linear momentum along the z direction simplifies the preceding equation to

$$\frac{\partial \pi}{\partial z} = -\sum \zeta_i e n_i \frac{\partial \psi}{\partial z}. \tag{13}$$

Now, if we take the differential of equation 11 with respect to ψ we find

$$\partial n_i = -\frac{\zeta_i e}{kT} n_i \partial \psi. \tag{14}$$

Thus, equation 13 can be expressed as

$$\frac{\partial \pi}{\partial z} = kT \sum \frac{\partial n_i}{\partial z}. \tag{15}$$

At this point, we make use of the classical demonstration of disjoining pressure – the additional pressure on the surface of the plates to keep the interlayer liquid in mechanical equilibrium as the plates are brought close to each other, as shown in Figure 1; we find the change in pressure at the plate surface on bringing two plates together from infinity to a separation, h, to be

$$(\pi_h)_{z=h/2} - (\pi_\infty)_{z=\infty/2} = kT\left(\sum \left(n_{i_h}\right)_{z=h/2} - \sum \left(n_{i_\infty}\right)_{z=\infty/2}\right). \tag{16}$$

which is the well-known "contact-value-theorem." Here, the subscripts h and ∞ denote the plate separation, and subscripts $z = h/2$ and $z = \infty/2$ denote the distance to the plate surfaces from the midplane in the positive z direction. By choosing ∞ as the reference state, since the disjoining pressure on the plates is zero when the plates are apart, i.e. $(\pi_\infty)_{z=\infty/2} = 0$, we can ultimately write

$$(\pi_h)_{z=h/2} = kT\left(\sum \left(n_{i_h}\right)_{z=h/2} - \sum \left(n_{i_\infty}\right)_{z=\infty/2}\right). \tag{17}$$

Thus, disjoining pressure due to the electrostatic effect arises from the increase in the number density of ions at the surfaces – more specifically the plate-solution contact interfaces– when the plates are brought close to each other. The right hand side of the above equation is a statement of osmotic pressure attributed to the difference in the ion number densities between the interlayer and the bulk liquid. Therefore, disjoining pressure may be understood as the mechanical, osmotic pressure at the surfaces required to counteract the gradient of electric potential – i.e., the z component of the electric field. The change in disjoining pressure is repulsive when there is an overall increase in the ion density at the surfaces due to the increased electrostatic effect compared to the bulk solution, and attractive

(1) An electrodynamic, or time-varying electric field introduces an additional linear momentum term and requires the inclusion of magnetodynamic terms since the coupling between electrodynamics and magnetodynamics means that they are always co-present. Here, we consider only an electrostatic field for simplicity since it is sufficient to explain the critical concepts.

(2) We assume that the liquid in the thin film retains the properties of bulk liquid and is sufficiently far away from interfaces to neglect surface forces. If one is interested in including surface forces, they can consider a separate force vector and the presumption of the sphericity of the Cauchy stress tensor is still valid.

when the ion density decreases as the plates are brought together. Researchers have long recognized the osmotic nature of the electrostatic repulsive force (see, e.g., [Coussy, 2010a, Derjaguin and Landau, 1941, Israelachvili, 2011]), and Coussy [2010b] noted the equivalency between what has been called disjoining pressure and osmotic pressure. However, the derivation herein seems to be the first to show the equivalence via the requirement for conservation of linear momentum. The ion density at the plate-liquid interface can decrease due to the binding of counterions to surfaces as plates are brought close to each other, especially in the presence of high concentrations of divalent and trivalent ions, which may even lead to complete neutralization and charge reversal of surfaces [Israelachvili, 2011]. If one is to consider the interaction of the charged particles with the counterions in the solution, one can still do that within the framework presented here. The derivation here can be modified to account for the adsorption or binding of counterions to the plate surface and the subsequent influence on the electric potential and electric field at the contact surface as the separation distance is reduced, allowing the existence of the Stern layer with varying thickness and the electric double layer (EDL). Quantification of the disjoining pressure from equation 17 requires the determination of ion number density as a function of the electrostatic potential at the plate surfaces. For a simplified case this can be done by using the Poisson-Boltzmann (PB) equation for a fixed surface charge density or surface potential. Let us now express Coulomb's law as

$$q_e = \varepsilon \mathrm{div}[\underline{E}], \tag{18}$$

where ε is the material permittivity, and apply $\underline{E} = -\mathrm{grad}\,[\,\psi]$, to reproduce Poisson's equation as

$$\mathrm{div}[\mathrm{grad}\,[\,\psi]] = -\frac{q_e}{\varepsilon}. \tag{19}$$

For a one-dimensional electric field in a monovalent 1:1 electrolyte solution between two plates, such as the one shown in Figure 2, equation 17 simplifies to

$$\begin{aligned}(\pi_h)_{z=h/2} =& kT\left(\left(n_{+_h}\right)_{z=h/2} + \left(n_{-_h}\right)_{z=h/2}\right) \\ &- kT\left(\left(n_{+_\infty}\right)_{z=\infty/2} + \left(n_{-_\infty}\right)_{z=\infty/2}\right),\end{aligned} \tag{20}$$

and we can stipulate that the potential does not vary along the x and y directions and, using equation 10, we write the one dimensional PB equation in the Cartesian coordinate system as

$$\frac{\partial^2 \psi}{\partial z^2} = -\frac{e}{\varepsilon}\left(n_+ - n_-\right) \tag{21}$$

Upon integration of equation 21 for a constant surface charge density, we find, with some mathematical manipulation, that

$$\begin{aligned}&kT\left(\left(n_{+_h}\right)_{z=h/2} + \left(n_{-_h}\right)_{z=h/2}\right) \\ &- kT\left(\left(n_{+_\infty}\right)_{z=\infty/2} + \left(n_{-_\infty}\right)_{z=\infty/2}\right) \\ &= kT\left(\left(n_{+_h}\right)_{z=h/2} + \left(n_{-_h}\right)_{z=h/2} - 2n_0\right).\end{aligned} \tag{22}$$

The above relationship arises from the hypothesis that the surface charge density, q_s, remains constant, i.e., the electric field at the contact surfaces is independent of the separation distance, and no counterions are adsorbed to the surfaces as the plates are pushed close to each other. Such assumption allows us to neglect the effect of charge regulation (i.e., counterion binding as plate separation decreases) and Stern layer on the electric field at the contact surface. Note that this assumption is introduced here as a boundary condition only to solve the PB equation. If one is to consider surface charge densities as a function of plate separation, they can still do it by introducing appropriate governing equation and boundary conditions for the electric potential profile to account for the drop in the surface potential due to ion binding. For instance, Ninham and Parsegian [1971] described an approach of solving the PB equation self-consistently for changing surface charge densities or electrostatic potentials. When counterions do not adsorb to the surfaces as the plates become close to each other and the surface densities remain the same, osmotic pressure at the surface is identical to that in the midplane. In other words, the intensity of the electrostatic effects at the surfaces in close proximity compared to that when the plates are infinitely apart is equal to the intensity of the electrostatic effects at the midplane. Substitution of equation 22 in equation 20 gives the disjoining pressure as

$$(\pi_h)_{h/2} = kT\left(\left(n_{+_h}\right)_{z=h/2} + \left(n_{-_h}\right)_{z=h/2} - 2n_0\right). \tag{23}$$

For two plates – with constant surface charge densities – separated by a thin liquid layer containing monovalent ions and counterions, disjoining pressure deduced here using the conservation of linear momentum yields the same form derived by Coussy [2010a] for the excess of internal pressure to explain the swelling of clay particles in fresh or salty water.

3. Validation and discussion

Equation 17 was evaluated by the osmotic pressure measurements found in literature for charged bilayers in dilute solution. In their experiment, Dubois et al. [1992] equilibrated the pure lamellar didodecyldimethylamonium bromide (DDAB)-water solution system at fixed osmotic pressure and salt chemical potential with a large reservoir containing dilute salt solution. The two solution systems were separated by a dialysis membrane permeable to solvent and ions. Chemical potential of the solvent in the reservoir was reduced by adding Dextran 500, a non-charged hydrophilic polymer, and KBr, and the resulting swelling was measured in terms of the interlamellar distances using small-angle neutron scattering. The lamellar particles were measured to bear a positive charge density of $0.235\mathrm{Cm}^{-2}$, equivalent to one charge per $0.68\mathrm{nm}^2$ [Dubois et al., 1992]. Figure 3b plots the osmotic pressure measurements for the DDAD-water system containing KBr concentrations of $c_0 = 10^{-3}$M and in the bulk (reservoir) solution.

In order to validate the general derivation of the preceding section before extending the theory to concrete, the

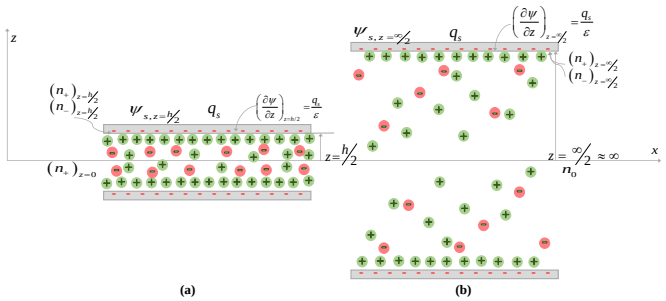

Figure 2. Distribution of co-ions and counterions between two charged surfaces, with surface potential of ψ_s and surface charge density of q_s per unit surface area, are (a) separated by a distance h and (b) infinitely apart from each other. n_+ and n_- are the number density (in units of m^{-3}) of cations and anions, respectively. n_0 presents the number density of ions in the bulk solution where the number of cations and anions are the same due to overall charge neutrality. Subscripts $z = h/2$ and $z = \infty/2$ represent the location at the plate surface when they are h distance apart and infinitely far apart, respectively; subscript $z = 0$ denotes the midplane.

lamellar particles from the experiments of Dubois et al. [1992] were modeled as flat plates as shown in Figure 3a, and the electrostatic potential, ψ, in the interlayer solution was determined by solving the PB equation numerically using the finite element method. The relative electrostatic permittivity of the salt solution was 78.5 at 298 K and the vacuum permittivity was $8.854 \times 10^{-12} C^2 J^{-1} m^{-1}$ so that $\varepsilon = 78.5 \times 8.854 \times 10^{-12} = 6.947 \times 10^{-10} C^2 J^{-1} m^{-1}$. The concentration c_0 is related to the ion number density n_0 by the relationship $n_0 = N_A c_0$, where $N_A = 6.022 \times 10^{23} mol^{-1}$ is the Avogadro number. Further, we consider a Boltzmann constant of $k = 1.381 \times 10^{-23} JK^{-1}$ and $T = 293K$. Since, in the bulk solution the ions are always paired up with counterions resulting in an overall charge neutrality, no electrostatic effect occurs, and $\psi_0 \approx 0$.

Because the PB equation is highly nonlinear resulting from the exponential dependence of ion density on the electrostatic potential, obtaining the exact analytical solution to this equation is not feasible. With the help of Debye-Huckel linearization, problems for low potential cases have been simplified for plate like particles to obtain approximate analytical solutions [Derjaguin and Landau, 1993, Verwey, 1947]. For planar geometry, exact solutions to the nonlinear PB equations also exist for symmetric and asymmetric electrolyte solutions [Andrietti et al., 1976, Chapman, 1913, Gouy, 1910, Grahame, 1953]. A few studies have presented analytical solutions to describe electrostatic potential between two similarly charged particles in terms of complex integrals [Coussy, 2010a, Polat and Polat, 2010, Saboorian-Jooybari and Chen, 2019, Zhang et al., 2018]. However, approximate solutions are generally only sufficiently accurate for surface separations beyond about one Debye length (please see [Israelachvili, 2011] for the definition and interpretation of Debye length), and one needs to seek numerical solutions [Anandarajah and Chen, 1994, Bohinc et al., 2016, Brumleve and Buck, 1978, Gross and Osterle, 1968, Olivares and McQuarrie, 1975, Ramanathan, 1983] for problems with complex geometry and high surface charge densities. For the problem in hand, the electrostatic potential, ψ, is computed numerically using the Mathematica function NDSolve with a discretized, finite element representation of the plate geometry; the solution is first obtained for dimensionless electric potential, $\varphi = \frac{e\psi}{kT}$, and then converted to the dimensional quantity.

The disjoining pressure was reproduced in Figure 3b using equation 20 for bulk salt concentrations of 10^{-3}M and 10^{-2}M, which is identical to the solution obtained from equation 23, the osmotic pressure at the midplane. Disjoining pressure for the bulk concentration of 1.5×10^{-3}M is also shown as the membrane was reported to release Na+ ions at a mean concentration of 0.5×10^{-3}M in the reservoir [Dubois et al., 1992]. The simulated results were found to be in very good agreement with the experimental measurements. As the bulk salt concentration was increased, the osmotic pressure in the liquid layer between the two plates decreased due to the reduced electric field magnitude – the negative gradient of the electric potential between the thin layer and the bulk solution; as a result, the disjoining pressure decreased.

Agreeable conclusions were also reached for the direct measurements of osmotic pressure in electrolyte solutions [Horn et al., 1988, Israelachvili and Adams, 1978]; between lipid bilayers [Cowley et al., 1978]; between silica surfaces [Ducker et al., 1991, Peschel et al., 1982]; and between mica surfaces [Horn et al., 1988, Kjellander et al., 1990]. The remarkably good agreement of the electrostatic forces with the experimental results indicates that the dielectric constant of water is close to the bulk value for surface separations as low as 2 nm, and below about 8 nm the electrostatic forces behave as if the surface charges are smeared out [Israelachvili, 2011]. Otherwise, significant deviations would have occurred, invalidating the treatment of the interlayer system as continuum.

The proposed derivation of disjoining pressure due to electrostatic forces can help explain the swelling of clay sheets, micelles, bilayers or colloid particles in pure water or dilute salt solutions down to below 10 nm. It does not include the attractive van der Waals forces or other short range surface forces. Measurements of forces between mica surfaces in the range of 1 – 100 nm showed that the attractive van der Waals forces are mostly active in the range of 1 – 15 nm; at above 6.5 nm the retardation sets in; and the attractive forces decay rapidly with increasing separations [Israelachvili and Adams, 1978]. The same study also reported the presence of an additional repulsive force with a characteristic decay length of 0.95±0.20 nm. These additional forces, further investigated by Pashley and his colleagues [Kjellander et al., 1990, Pashley, 1981b, Pashley and Quirk, 1984], are indeed very important for complex colloidal and biological systems where these forces govern the short-range interactions – below 6 nm, however can be omitted for interactions at or above 10 nm.

Further, this preceding formulation gives insight into the effect of disjoining pressure in problems other than the example (two parallel plates) examined herein. For instance, Wasan and Nikolov [2003] reported an unexpected observation where the addition of electrolytes in the aqueous micellar solution, despite the reduction of the interfacial tension between the oil and aqueous solution that is believed to stimulate the separation process, reduced the detachment of the oil drop from the glass surface. Such a phenomenon – observed at the same range of surface separations examined here – may be attributable to the reduction of the osmotic pressure – of electrostatic origin – with the added electrolytes, which diminishes the disjoining pressure and subsequently the detachment of the drop.

It is important to recognize that the disjoining pressure in the preceding example only changes when the surface separation distance between the plates change. As noted previously, since the pore sizes in drying concrete are not anticipated to change significantly during the drying process, there is effectively no change in the separation distance between the solid particles. Does this mean that disjoining pressure changes are not a mechanism contributing to concrete shrinkage? Second, what is the relevance of the preceding analysis to concrete shrinkage? To answer these questions, let us consider the morphology of cement hydrates of a matured cement paste and its pore network.

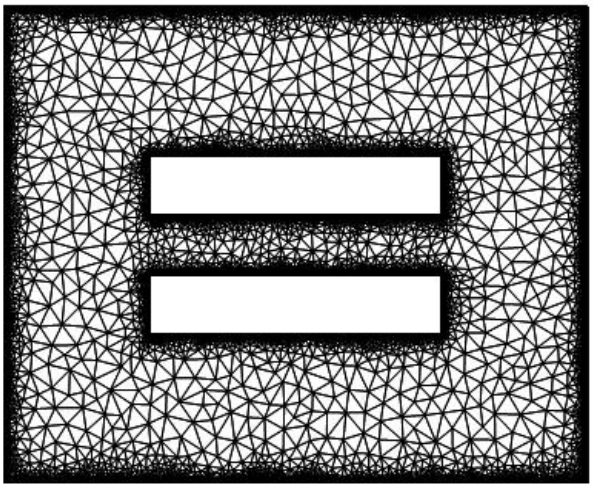

(a) Geometry and mesh

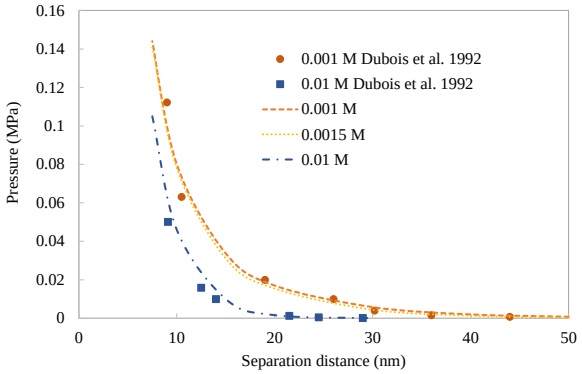

(b) Disjoining pressure

Figure 3. (a) Geometry and mesh for the finite element analysis of the Poisson-Boltzmann (PB) model for electrolyte solution between two planar charged surfaces. (b) Disjoining pressure, namely the excess of osmotic pressure at the plate surface separated by solution which is in equilibrium with a bulk solution containing ion concentrations of 10^{-3}M and 10^{-2}M. The circular and the square markers plot the experimental results obtained by Dubois et al. [1992]. Dashed and dotted lines reproduce the disjoining pressure obtained by equation 17 and solved for the PB model for an 1:1 electrolyte solution.

4. Implications in drying shrinkage of cementitious materials

When cement is mixed with water, anhydrous calcium and silicate oxides react with water to form tricalcium silicate solution. With the increased pH, this solution becomes supersaturated and forms nanoplatelets of C-S-H with typical dimensions of 60 nm x 30 nm x 5 nm [Jönsson et al., 2004, Labbez et al., 2006]. Jennings [2008] treats C-S-H as assembly of "globules" of small brick like particles, which consist of solid C-S-H with a cross-section thickness of 5 nm and internal water. Muller et al. [2013] have used ^{1}H relaxation nuclear magnetic resonance (NMR) measurements to picture C-S-H morphology as a function of hydration degree for a range of water to cement ratios of cement paste. The experiments show that as the hydration progresses C-S-H grows as a loose-packed assembly of nanocrystalline regions. In these regions the calcium silicate layers are stacked with interlayer water (~ 1 nm in size) and are interspersed with gel pores with a characteristic size of 3-5 nm that remain relatively constant [Muller et al., 2013]. The NMR data show that the gel porosity and the gel pore size reach a plateau after 1-2 days of hydration, whereas the volume of hydrates continuously grows. The interhydrate pores containing the free water stabilizes at around 8-10 nm, and these pores are not intrinsic to the C-S-H hydrates. The interhydrate pores are comparable in size to the large globule pores suggested by Jennings [2008]. The solid C-S-H density without the gel pores decreases very slightly with the degree of hydration. The bulk C-S-H density that includes the gel water, on the other hand, increases markedly during hydration from around 1.8 g/cm^3 at 1 day to 2.65 g/cm^3 at 1 year. Muller et al. [2013] suggested that the C-S-H aggregates of layers are approximately 4.2 nm thick, which is close to the globule size suggested by [Jennings, 2008].

These C-S-H particles become highly negatively charged and are mainly counterbalanced by divalent calcium counterions. The surface density of ionized sites is reported to be in the range of $2.5-5$ nm^{-2}, with a surface charge density of $0.4-0.8$ C/m^2 [Jönsson et al., 2004]. For two C-S-H globules separated by 2 nm, the concentration of the counter-ions

confined in the vicinity of the surfaces is believed to be 2 M compared to the bulk concentration of 0.002 M [Jönsson et al., 2004]. As the hydrated cement paste is subject to drying, the liquid saturation within the pore space decreases and the concentration of dissolved species in the bulk pore liquid increases. Grasley and Leung [2011] constructed desorption isotherms for materials with varying water to cement ratios (w/c) and age from the measured mass loss data (see Figure 4b). This desorption isotherm can be used to extrapolate bulk concentrations of the pore liquid at decreasing liquid saturation levels during the drying process.

For simulating the effect of disjoining pressure in drying shrinkage of cementitious materials, we consider two C-S-H aggregates with a stack thickness of 5 nm and width of 30 nm, as shown in Figure 4a, separated by 10 nm in a continuum characterized by a relative permittivity of 78.5. The model adopted here is a simplistic view of C-S-H aggregates and does not represent individual C-S-H particles packed with interlayer and gel water. Simulation of complex C-S-H structures where C-S-H particles are closely packed and are separated by interlayer water and gel water, is still possible under the framework of finite element analysis but is computationally rather expensive. Moreover, if a range of pore sizes from ~ 1 to 10 nm are to be simulated representing interlayer water, gel water, and interhydrate pores, short range surface forces which have been excluded from our simulation, can no longer be excluded. With the simplistic geometry, the modeled results provide the general trend and extend Derjaguin's concept of disjoining pressure to the context of drying shrinkage of cementitious materials.

We presume the paste is fully matured so that the C-S-H densification plateaus and there is no notable change in the pore spacing due to the drying process, rather the pore space is gradually invaded by the air filled with vapor. Therefore, the simulated surface separation of the C-S-H aggregates remains constant throughout the drying process. We assume that the charge on the C-S-H aggregates is uniformly smeared out with a density of 0.8 C/m2. The initial concentration of the bulk solution is assumed to be 0.002 M for a relative humidity of 100%, such that the matured cement paste is fully saturated. This initial value of relative humidity is also chosen as the reference state where the shrinkage is considered "zero." Thus, shrinkage stress due to the disjoining pressure mechanism is defined as the difference in the disjoining pressure from the reference state to that at any point with lower relative humidity. Ionic concentrations in the bulk pore liquid with respect to varying relative humidity are extrapolated from the desorption isotherm for hydrated cement paste with w/c of 0.4 at the age of 7 days, as shown in Figure 4b. Saturation values corresponding to relative humidity lower than 25% have been obtained by hypothetically extending the S-RH curve to 0, as shown by the solid line in Figure 4b. The disjoining pressure is calculated for a series of discrete concentrations, with each calculation performed at steady state. Similar to the previous example, the disjoining pressure at the C-S-H surface has been simulated for varying concentration of the bulk pore liquid by solving the PB equation using a finite element model and presented in Figure 4c.

As the relative humidity decreases, the liquid water leaves the pore solution increasing the concentration of counterions in the bulk solution. As a result, in the film separating the C-S-H aggregates and the bulk solution, the gradient in electrical potential in the direction perpendicular to the interparticle gap decreases, decreasing the magnitude of the repulsive disjoining force. In turn, this increases the magnitude of the shrinkage stress. Thus, the contribution of disjoining pressure in drying shrinkage is osmotic in nature and does not require changes in the interparticle gap.

Similarly, one can simulate the effect of water curing on hydrated cement paste by considering the unsaturated or partially saturated hydrated cement paste as the starting point and slowly increasing the liquid saturation thereafter. If one immerses a partially saturated hydrated cement paste such that the liquid saturation of the specimen is about 0.4 for instance, into pure water, the water gradually invades the empty dried pores. As the water penetrates the pore network and water saturation increases to 1 (in this case the x-axis in Figure 4c is reversed), the water dilutes the salt in big pores, ultimately increasing the difference between the salt concentration in the bulk liquid (in big pores) and in the gap between the charged particles. The increased gradient in electric potential perpendicular to the direction of interparticle gap increases the disjoining pressure, and as a result the hydrated cement paste expands when cured in pure water.

Further, one can easily show that the magnitude of shrinkage stress presented in Figure 4c is small compared to the pressure calculated using the Lewis equation (equation 3), and capillary pressure plays the dominant role in inducing shrinkage of cementitious materials even at very low relative humidity. The relative contribution of these two mechanisms may be quantitatively assessed by considering the weighted average of the capillary pressure and disjoining pressure as outlined by El Tabbal et al. [2020] within the framework of poromechanics [Coussy, 2010c].

It is necessary to recognize that the geometry in Figure 4a, which assumes a bulk solution surrounding the two surfaces in close proximity to each other, breaks down at low saturation levels. This means that the predicted disjoining pressures at low degrees of saturation are less reliable when the ionic concentration is induced by drying. However, the general trend of decreasing disjoining pressure (increasing shrinkage stress) should yet hold. In addition, the modeled geometry is essentially one dimensional because the plates are long relative to the separation distance. In reality, the electrostatic field is a vector and acts in three dimensions. By combining equations 5, 9, and 21 one finds that, for a 2D (x and z) Cartesian coordinate system,

$$\frac{\partial \pi}{\partial z} = \varepsilon E_z \left(\frac{\partial E_x}{\partial x} + \frac{\partial E_z}{\partial z} \right). \tag{24}$$

If the z direction is in line with the separation between two surfaces (i.e., perpendicular to the two parallel surfaces), it is clear that the disjoining pressure is generally a function of the electric field in the direction perpendicular

and parallel to the surfaces (x direction). For surfaces that approximate two parallel, infinite plates, the function simplifies to $\partial\pi = \varepsilon\,(E_z \partial E_z)$ and becomes one-dimensional (like the lamellar particles of the previous example). However, for surfaces that are not approximated by infinite plates (e.g., spherical or cubic particles), the term involving E_x does not become zero. Furthermore, while E_z tends to vary only with changing separation distance between the surfaces, for realistic shaped particles of calcium-silicate-hydrate (C-S-H), E_x may well vary due to changes in ionic concentrations of the bulk liquid adjacent to the gap between the particles. Thus, given the shape and structure of calcium-silicate-hydrate particles in cementitious materials, it is necessary to account for the geometry in simulations and not discount the presence of the electrostatic field in directions other than perpendicular to the gap between particles. Considerations of C-S-H globules as 3D particles may yield different values of disjoining pressure from that obtained here, however its contribution compared to the capillary pressure is still anticipated to be small.

It should be noted here that simulated phenomenon of disjoining pressure changes associated with changes in bulk pore solution ionic concentration may also explain the significance of the presence of dissolved species on disjoining pressure, as observed in several studies investigating the disjoining pressure with surface apparatuses [Beltzung and Wittmann, 2005, Churaev et al., 2000, Pashley, 1981a,b, Peschel et al., 1982], and the swelling that occurs when cementitious materials are placed in pure water or a true 100% RH environment (above the equilibrium RH dictated by the water activity reduction of the pore solution due to dissolved salts).

5. Conclusions

Capillary pressure and disjoining pressure are generally believed to be the major driving force for drying induced shrinkage in cementitious materials. However, the relative contribution of the two mechanisms has been debated and not fully understood. This paper investigates the mechanism driving the disjoining pressure induced drying shrinkage of concrete. A continuum based approach for quantifying disjoining pressure in a thin liquid layer between two charged planar surfaces in a liquid bath has been described. This approach assumes that the thin liquid layer retains the properties of the bulk solution and a priori the sphericity of the Cauchy stress tensor of the interlayer liquid. Further, this approach uses conservation of linear momentum to derive disjoining pressure from the electrostatic Lorentz force vector to show that disjoining pressure in a solution between two solid surfaces is essentially the osmotic pressure at the charged surfaces, which is in agreement with historical references. The disjoining pressure offsets the linear momentum associated with the larger electric potential gradient compared to that in the bulk solution to achieve overall equilibrium. Simulations using the theory are in good agreement with the experimental measurements of osmotic pressure in the dilute solution of charged bilayers [Dubois et al., 1992]. We show the shrinkage stress in concrete due to disjoining pressure, defined as the difference between the disjoining pressure at the reference state with full relative humidity and that at a low relative humidity, is induced by the increased ionic concentration in the bulk pore solution caused by the removal of water upon drying and is osmotic in nature. In contrast to previous work on modeling disjoining pressure in concrete, our approach does not require significant changes to interparticle gaps during the drying process. Instead, the recognition of electrostatic field as a vector field where components of the field in directions perpendicular to the gap between the particles may contribute to disjoining pressure has led to a new understanding of the mechanism.

Conflicts of Interest

The authors declare no conflicts of interest. The complete review history is available online.

References

Anandarajah, A. and Chen, J. (1994). Double-layer repulsive force between two inclined platy particles according to the gouy-chapman theory. *Journal of Colloid And Interface Science*, 168(1):111–117.

Andrietti, F., Peres, A., and Pezzotta, R. (1976). Exact solution of the unidimensional poisson-boltzmann equation for a 1:2 (2:1) electrolyte. *Biophysical Journal*, 16(9):1121–1124.

Basu, S. and Sharma, M. (1996). Measurement of critical disjoining pressure for dewetting of solid surfaces. *Journal of Colloid and Interface Science*, 181(2):443–455.

Beltzung, F. and Wittmann, F. H. (2005). Role of disjoining pressure in cement based materials. *Cement and Concrete Research*, 35(12):2364–2370.

Bohinc, K., Volpe Bossa, G., Gavryushov, S., and May, S. (2016). Poisson-boltzmann model of electrolytes containing uniformly charged spherical nanoparticles. *The Journal of Chemical Physics*, 145(23).

Brumleve, T. R. and Buck, R. P. (1978). Numerical solution of the nernst-planck and poisson equation system with applications to membrane electrochemistry and solid state physics. *Journal of Electroanalytical Chemistry and Interfacial Electrochemistry*, 90(1):1–31.

Chapman, D. (1913). A contribution to the theory of electrocapillarity. *London, Edinburgh and Dublin Philosophical Magazine and Journal of Science*, 25(148):475.

Chatterjee, A., Plawsky, J. L., and Wayner, P. C. (2011). Disjoining pressure and capillarity in the constrained vapor bubble heat transfer system. *Advances in Colloid and Interface Science*, 168(1):40–49.

Chengara, A., Nikolov, A. D., Wasan, D. T., Trokhymchuk, A., and Henderson, D. (2004). Spreading of nanofluids driven by the structural disjoining pressure gradient. *Journal of Colloid and Interface Science*, 280(1):192–201.

Christenson, H. (1985). Capillary condensation in systems of immiscible liquids. *Journal of Colloid and Interface Science1*, 104(1):234–249.

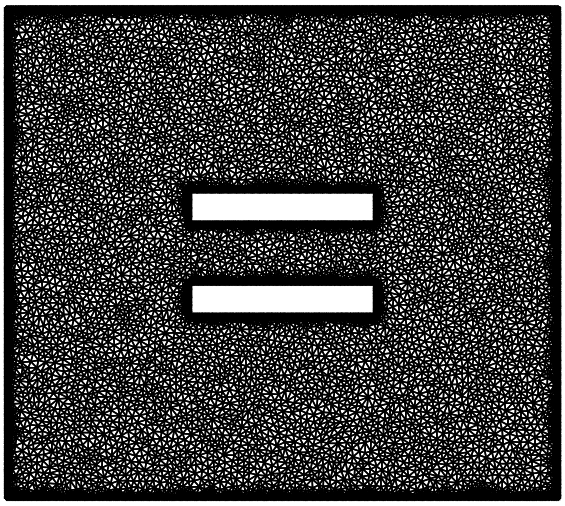

(a) Geometry and mesh

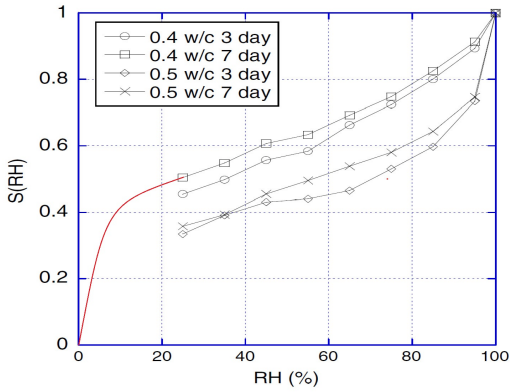

(b) Liquid saturation vs relative humidity

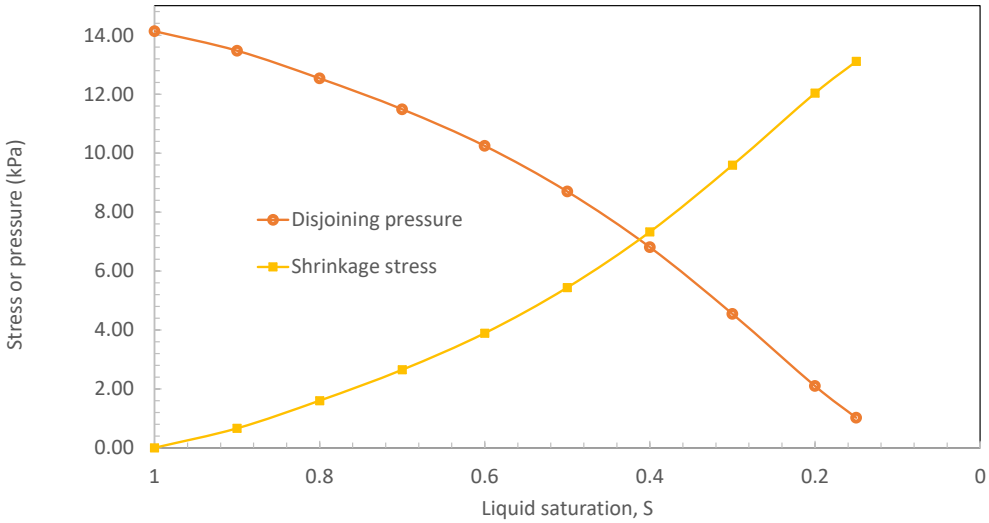

(c) Disjoining pressure and shrinkage stress vs liquid saturation

Figure 4. (a) Geometry and mesh for the finite element analysis of the for electrolyte solution between two planar charged surfaces. (b) Saturation as a function of relative humidity obtained from Grasley and Leung [2011]. The solid line hypothetically extends the "0.4 w/c 3 day" line to zero relative humidity (RH). (c) Shrinkage stress as a function of liquid saturation.

Christenson, H. (1988). Adhesion between surfaces in undersaturated vapors—a reexamination of the influence of meniscus curvature and surface forces. *Journal of Colloid and Interface Science1*, 121(1):170–178.

Churaev, V. N., Bardasov, S. A., and Sobolev, V. D. (1994). Disjoining pressure of thin nonfreezing water interlayers between ice and silica surface. *Langmuir*, 10(11):4203–4208.

Churaev, V. N., Setzer, M. J., Wowra, O., and Reick, M. (2000). Electrolytes in narrow pores / electrolyten in engen poren. *Restoration of Buildings and Monuments*, 6(1):87–102.

Coussy, O. (2010a). The disjoining pressure. In *Mechanics and Physics of Porous Solids*, pages 128–131. John Wiley & Sons Ltd, West Sussex.

Coussy, O. (2010b). Electrostatics and excess of osmotic pressure. In *Mechanics and Physics of Porous Solids*, pages 25–32. John Wiley & Sons Ltd, West Sussex.

Coussy, O. (2010c). *Mechanics and Physics of Porous Solids*. John Wiley & Sons Ltd.

Cowley, A. C., Fuller, N. L., Rand, R. P., and Parsegian, V. A. (1978). Measurement of repulsive forces between charged phospholipid bilayers. *Biochemistry (Easton)*, 17(15):3163–3168.

Derjaguin, B. and Churaev, N. (1978). On the question of determining the concept of disjoining pressure and its role in

the equilibrium and flow of thin films. *Journal of Colloid and Interface Science*, 66(3):389–398.

Derjaguin, B., Churaev, N., and Muller, V. (1987). *Surface forces*. Consultants Bureau, New York.

Derjaguin, B. and Kusakov, M. (1936). Properties of thin liquid layers. *Izv. Akad. Nauk SSSR, Ser. Khim.*, 5(5):741.

Derjaguin, B. and Kusakov, M. (1937). No title. *Izv. Akad. Nauk SSSR, Ser. Khim.*, 5:1119.

Derjaguin, B. and Kusakov, M. (1939). Anomalous properties of thin polymolecular films v. *Acta Physicochim. URSS*, 10(25).

Derjaguin, B. and Landau, L. (1941). Theory of the stability of strongly charged lyophobic sols and of the adhesion of strongly charged particles in solutions of electrolytes. *Progress in Surface Science*, 43:30–59.

Derjaguin, B. and Landau, L. (1993). Theory of the stability of strongly charged lyophobic sols and of the adhesion of strongly charged particles in solutions of electrolytes. *Progress In Surface Science*, 43:30–59.

Derjaguin, V. B. and Obukhov, E. (1936). Anomalien dunner flussig- keitsschichten iii. *Acta Physicochim. URSS*, 5(1).

Dubois, M., Zemb, T., Belloni, L., Delville, A., Levitz, P., and Setton, R. (1992). Osmotic pressure and salt exclusion in electrostatically swollen lamellar phases. *The Journal of chemical physics*, 96(3):2278–2286.

Ducker, W. A., Senden, T. J., and Pashley, R. M. (1991). Direct measurement of colloidal forces using an atomic force microscope. *Nature*, 353(6341):239–241.

El Tabbal, G., Dangla, P., Vandamme, M., Bottoni, M., and Granet, S. (2020). Modelling the drying shrinkage of porous materials by considering both capillary and adsorption effects. *Journal of the mechanics and physics of solids*, 142.

Fisher, L., Gamble, R., and Middlehurst, J. (1981). Capillary condensation in systems of immiscible liquids. *Nat1ure*, 290(5807):575–576.

Fisher, L. and Israelachvili, J. (1981a). Direct measurement of the effect of meniscus forces on adhesion: A study of the applicability of macroscopic thermodynamics to microscopic liquid interfaces. *Colloids and Surfaces*, 3(4):303–319.

Fisher, L. and Israelachvili, J. (1981b). Experimental studies on the applicability of the kelvin equation to highly curved concave menisci. *Journal of Colloid and Interface Science*, 80(2):528–541.

Gibbs, J. W. (1878). On the equilibrium of heterogeneous substances. *American Journal of Science*, s3-16(96):441–458.

Gor, G. Y. and Neimark, A. (2010). Adsorption-induced deformation of mesoporous solids. *Langmuir*, 26(16):13021–13027.

Gouy, M. (1910). Sur la constitution de la charge électrique à la surface d'un électrolyte. *J. Phys. Theor. Appl.*, 9(1):457–468.

Grahame, D. C. (1953). Diffuse double layer theory for electrolytes of unsymmetrical valence types. *The Journal of Chemical Physics*, 21(6):1054–1060.

Grasley, Z. C. and Leung, C. K. (2011). Desiccation shrinkage of cementitious materials as an aging, poroviscoelastic response. *Cement and Concrete Research*, 41(1):77–89.

Gross, R. J. and Osterle, J. F. (1968). Membrane transport characteristics of ultrafine capillaries. *The Journal of Chemical Physics*, 49(1):228–234.

Horn, R. G., Bachmann, D. J., Connor, J. N., and Miklavcic, S. J. (1996). The effect of surface and hydrodynamic forces on the shape of a fluid drop approaching a solid surface. *Journal of Physics: Condensed Matter*, 8(47):9483.

Horn, R. G., Evans, D. F., and Ninham, B. W. (1988). Double-layer and solvation forces measured in a molten salt and its mixtures with water. *The Journal of Physical Chemistry*, 92(12):3531–3537.

Hu, H. and Sun, Y. (2013). Molecular dynamics simulations of disjoining pressure effect in ultra-thin water film on a metal surface. *Applied Physics Letters*, 103(26).

Israelachvili, J. N. (2011). Chapter 14 - electrostatic forces between surfaces in liquids. In *Intermolecular and Surface Forces*, pages 291–340. Academic Press, San Diego.

Israelachvili, J. N. and Adams, G. E. (1978). Measurement of forces between two mica surfaces in aqueous electrolyte solutions in the range 0–100 nm. *Journal of the Chemical Society, Faraday Transactions 1: Physical Chemistry in Condensed Phases*, 74:975. 0300-9599.

Jennings, H. M. (2008). Refinements to colloid model of c-s-h in cement: Cm-ii. *Cement and Concrete Research*, 38(3):275–289.

Jönsson, B., Wennerström, H., Nonat, A., and Cabane, B. (2004). Onset of cohesion in cement paste. *Langmuir*, 20(16):6702–6709.

Kjellander, R., Marčelja, S., Pashley, R. M., and Quirk, J. P. (1990). A theoretical and experimental study of forces between charged mica surfaces in aqueous cacl2 solutions. *The Journal of Chemical Physics*, 92(7):4399–4407.

Kuchin, I., Matar, O., Craster, R., and Starov, V. (2014). Influence of the disjoining pressure on the equilibrium interfacial profile in transition zone between a thin film and a capillary meniscus. *Colloids and Interface Science Communications*, 1:18–22.

Labbez, C., Jönsson, B., Pochard, I., Nonat, A., and Cabane, B. (2006). Surface charge density and electrokinetic potential of highly charged minerals: Experiments and monte carlo simulations on calcium silicate hydrate. *Journal of Physical Chemistry B*, 110(18):9219–9230.

LANDAU, L. and LIFSHITZ, E. (1984). Chapter i - electrostatics of conductors. In LANDAU, L. and LIFSHITZ, E., editors, *Electrodynamics of Continuous Media (Second Edition)*, volume 8 of *Course of Theoretical Physics*, pages 1–33. Pergamon, Amsterdam, second edition edition.

Langevin, D. (2000). Influence of interfacial rheology on foam and emulsion properties. *Advances in Colloid and Interface Science*, 88(1):209–222.

Laplace, P. (1805). *Traité de Mécanique Céleste*, volume 4. Imprimerie de Crapelet.

Lewis, G. N. (1901). The law of physico-chemical change. *Proceedings of the American Academy of Arts and Sciences*, 37(3):49–69.

Mate, C. (1992). Application of disjoining and capillary pressure to liquid lubricant films in magnetic recording. *Journal of Applied Physics*, 72(2):3084–3090.

Maxwell, J. (1954). *A Treatise on Electricity and Magnetism (Third Edition)*. Dover Publications, Inc., New York, third edition edition.

Muller, A. C. A., Scrivener, K. L., Gajewicz, A. M., and McDonald, P. J. (2013). Densification of c–s–h measured by 1h nmr relaxometry. *Journal of physical chemistry. C*, 117(1):403–412.

Napari, I. and Laaksonen, A. (2003). Disjoining pressure of thin films on spherical core particles. *The Journal of Chemical Physics*, 119(19):10363–10366.

Neimark, A., Ravikovitch, P., and Vishnyakov, A. (2003). Bridging scales from molecular simulations to classical thermodynamics: density functional theory of capillary condensation in nanopores. *Journal of Physics Condensed Matter*, 15:347–365.

Ninham, B. W. and Parsegian, V. (1971). Electrostatic potential between surfaces bearing ionizable groups in ionic equilibrium with physiologic saline solution. *Journal of Theoretical Biology*, 31(3):405–428.

Olivares, W. and McQuarrie, D. (1975). On the theory of ionic solutions. *Biophysical Journal*, 15(2):143–162.

Pashley, R. M. (1981a). Dlvo and hydration forces between mica surfaces in li+, na+, k+, and cs+ electrolyte solutions: A correlation of double-layer and hydration forces with surface cation exchange properties. *Journal of Colloid and Interface Science*, 83(2):531–546.

Pashley, R. M. (1981b). Hydration forces between mica surfaces in aqueous electrolyte solutions. *Journal of Colloid and Interface Science*, 80(1):153–162.

Pashley, R. M. and Quirk, J. P. (1984). The effect of cation valency on dlvo and hydration forces between macroscopic sheets of muscovite mica in relation to clay swelling. *Colloids and Surfaces*, 9(1):1–17.

Peschel, G., Belouschek, P., Müller, M. M., Müller, M. R., and König, R. (1982). The interaction of solid surfaces in aqueous systems. *Colloid and Polymer Science*, 260(4):444–451.

Picano, F., Oswald, P., and Kats, E. (2001). Disjoining pressure and thinning transitions in smectic-a liquid crystal films. *Physical Review E*, 63(2).

Plassard, C., Lesniewska, E., Pochard, I., and Nonat, A. (2005). Nanoscale experimental investigation of particle interactions at the origin of the cohesion of cement. *Langmuir*, 21(16):7263–7270.

Polat, M. and Polat, H. (2010). Analytical solution of poisson-boltzmann equation for interacting plates of arbitrary potentials and same sign. *Journal of colloid and interface science*, 341(1):178–185.

Pushkarova, R. A. and Horn, R. G. (2005). Surface forces measured between an air bubble and a solid surface in water. *Colloids and Surfaces A: Physicochemical and Engineering Aspects*, 261(1):147–152.

Pushkarova, R. A. and Horn, R. G. (2008). Bubble-solid interactions in water and electrolyte solutions. *Langmuir : the ACS journal of surfaces and colloids.*, 24(16).

Rahman, S. F. and Grasley, Z. C. (2017). The significance of pore liquid pressure and disjoining pressure on the desiccation shrinkage of cementitious materials. *International Journal of Advances in Engineering Sciences and Applied Mathematics*, 9(2):87–96.

Ramanathan, V. G. (1983). Statistical mechanics of electrolytes and polyelectrolytes. iii. the cylindrical poisson–boltzmann equation. *The Journal of Chemical Physics*, 78(6):3223–3232.

Saboorian-Jooybari, H. and Chen, Z. (2019). Analytical solutions of the poisson-boltzmann equation within an interstitial electrical double layer in various geometries. *Chemical Physics*.

Scherer, G. W. (2015). Drying, shrinkage, and cracking of cementitious materials. *Transport in Porous Media*, 110(2):311–331.

Sefiane, K. (2006). On the role of structural disjoining pressure and contact line pinning in critical heat flux enhancement during boiling of nanofluids. *Applied Physics Letters*, 89(4).

Starov, V. M., Kalinin, V. V., and Ivanov, V. I. (1994). Influence of surface forces on hydrodynamics of wetting. *Colloids and Surfaces A: Physicochemical and Engineering Aspects*, 91:149–154.

Stubenrauch, C. and Von Klitzing, R. (2003). Disjoining pressure in thin liquid foam and emulsion films - new concepts and perspectives. *Journal of Physics Condensed Matter*, 15(27).

Thomson, W. (1871). On the equilibrium of vapour at a curved surface of liquid. *Philosophical Magazine*, 4:448–452.

Verwey, E. J. (1947). Theory of the stability of lyophobic colloids. *Journal of Physical and Colloid Chemistry*, 51(3):631–636.

Wasan, D. T. and Nikolov, A. D. (2003). Spreading of nanofluids on solids. *Nature*, 423:156+.

Yaminsky, V. V., Ohnishi, S., Vogler, E. A., and Horn, R. G. (2010). Stability of aqueous films between bubbles. part 1. the effect of speed on bubble coalescence in purified water and simple electrolyte solutions. *Langmuir*, 26(11):8061–8074.

Yang, Q., Sun, P. Z., Fumagalli, L., Stebunov, Y. V., Haigh, S. J., Zhou, Z. W., Grigorieva, I. V., Wang, F. C., and Geim, A. K. (2020). Capillary condensation under atomic-scale confinement. *Nature*, 588(7837):250–253.

Young, T. (1805). An essay on the cohesion of fluids. *Philosophical Transactions of the Royal Society of London*, 95:65–87.

Zhang, W., Wang, Q., Zeng, M., and Zhao, C. (2018). An exact solution of the nonlinear poisson-boltzmann equation in parallel-plate geometry. *Colloid and Polymer Science*, 296(11):1917–1923.

Manuscript received 7th February 2023, revised and accepted 5th April 2023.